Published in final edited form as:
Biochem J. 2013 May 1; 451(3): 375–388. doi:10.1042/BJ20121344.

PDGF-mediated autophagy regulates vascular smooth muscle cell phenotype and resistance to oxidative stress

Joshua K. Salabei[*,†], **Timothy D. Cummins**[*], **Mahavir Singh**[*], **Steven P. Jones**[*,‡], **Aruni Bhatnagar**[*,†,‡], and **Bradford G. Hill**[*,†,‡]

[*]Diabetes and Obesity Center and Institute of Molecular Cardiology, University of Louisville School of Medicine, Louisville, KY 40202

[†]Department of Biochemistry and Molecular Biology, University of Louisville School of Medicine, Louisville, KY 40202

[‡]Department of Physiology and Biophysics, University of Louisville School of Medicine, Louisville, KY 40202

SYNOPSIS

Vascular injury and chronic arterial diseases result in exposure of vascular smooth muscle cells (VSMCs) to increased concentrations of growth factors. The mechanisms by which growth factors trigger VSMC phenotype transitions remain unclear. Because cellular reprogramming initiated by growth factors requires not only the induction of genes involved in cell proliferation but also the removal of contractile proteins, we hypothesized that autophagy is an essential modulator of VSMC phenotype. Treatment of VSMCs with platelet-derived growth factor (PDGF)-BB resulted in decreased expression of the contractile phenotype markers calponin and α-smooth muscle actin and upregulation of the synthetic phenotype markers osteopontin and vimentin. Autophagy, as assessed by LC3-II abundance, LC3 puncta formation and electron microscopy, was activated by PDGF exposure. Inhibition of autophagy with 3-methyladenine, spautin-1, or bafilomycin stabilized the contractile phenotype. In particular, spautin-1 led to a remarkable stabilization α-smooth muscle cell actin and calponin in PDGF-treated cells and prevented actin filament disorganization, diminished production of extracellular matrix and abrogated VSMC hyperproliferation and migration. Interestingly, treatment of cells with PDGF prevented protein damage and cell death due to exposure to the lipid peroxidation product, 4-hydroxynonenal. These results demonstrate a distinct form of autophagy induced by PDGF that is essential for attaining the synthetic phenotype and for survival under conditions of high oxidative stress found to occur in vascular lesions.

Corresponding Author: Bradford G. Hill, Ph.D., Diabetes and Obesity Center, Institute of Molecular Cardiology, University of Louisville, 580 S. Preston St., Rm 404A, Louisville, KY, 40202; Tel: (502) 852-1015, Fax: (502) 852-3663, bradford.hill@louisville.edu.

AUTHOR CONTRIBUTION

Josh Salabei designed and performed the experiments, analyzed data and helped write the paper; Timothy D. Cummins helped perform experiments and analyze data; Mahavir Singh helped standardize experiments using GFP-LC3 vectors; Steven Jones provided reagents, materials, and guidance for confocal imaging experiments as well as help write the paper; Aruni Bhatnagar helped to design experiments, analyze data and write the paper; and Bradford Hill designed experiments, analyzed data, and wrote the paper.

Keywords

autophagy; atherosclerosis; restenosis; 4-hydroxynonenal; growth factor; spautin

INTRODUCTION

Vascular smooth muscle cells (VSMCs) are essential regulators of vascular function. In healthy arteries, VSMCs are located in the medial vascular layer, where they express contractile proteins that help to regulate vessel tone and blood flow [1]. During atherogenesis and arterial restenosis, VSMCs change from a contractile phenotype to a synthetic phenotype. This promotes their migration to the intima, increases their proliferative capacity, and promotes the synthesis of extracellular matrix proteins [2]. These changes in VSMC phenotype appear to be fundamental in regulating the composition and stability of vascular lesions [3].

While several factors may mediate VSMC phenotype transitions, platelet-derived growth factor (PDGF) is among the most robust phenotype-modulating agents and has been shown to be a primary regulator of smooth muscle cell growth and proliferation. Antibodies against PDGF [4–6] or PDGF receptors [7, 8], antisense oligonucleotides to PDGF receptors [9, 10], or PDGF aptamers [11] inhibit smooth muscle accumulation in the intima after balloon injury, and VSMCs lacking PDGFR-β show strikingly diminished neointimal accumulation after carotid artery ligation [12]. Moreover, pharmacological inhibition of PDGF signaling reduces VSMC proliferation, migration, and occupancy in the neointima [13–15]. Hence, understanding how PDGF regulates VSMC phenotype may be essential for developing better and more targeted strategies for preventing or ameliorating vascular disease.

The switch from the contractile to the synthetic VSMC phenotype caused by PDGF is initiated upon PDGF binding to surface receptors, which activate several intracellular signaling pathways that ultimately regulate gene expression and cellular function. These signaling pathways have been shown to result in decreased abundance of contractile proteins and increased expression of synthetic proteins such as osteopontin [1, 16] and vimentin [17, 18]. Such structural changes have been shown to be prerequisites for enhanced cellular proliferation of VSMCs in culture [19]. Although multiple studies have focused on identifying the molecular mechanisms involved in phenotype switching [1, 2], it remains unclear how VSMCs can rapidly change from the contractile to the synthetic phenotype. Previous work from our laboratory has shown that autophagy is activated in VSMCs to remove oxidatively damaged proteins [20], which can form large aggregates that can be particularly difficult to proteolyze. This suggested to us that the contractile apparatus, which must be removed during cellular transition to the synthetic phenotype, may also be degraded by autophagy and that autophagy might be an essential regulator of VSMC viability in diseased vessels. Therefore, we examined whether PDGF-induced transition from the contractile to the synthetic phenotype is accompanied by an increase in autophagy and whether stimulation of autophagy is required for phenotype switching. Our results support the notion that autophagy is essential for the conversion of VSMC from a contractile to a

synthetic phenotype and that this increase in autophagy in synthetic cells could also function to prevent cell death due to oxidative stress.

EXPERIMENTAL

Materials

Antibodies against α-smooth muscle cell-actin (a-SMA), calponin and α-tubulin were purchased from Sigma-Aldrich (St. Louis, MO, USA). Osteopontin antibody was purchased from Santa Cruz biotechnology (Santa Cruz, CA, USA). Recombinant FGF-1 was obtained from eBiosciences (San Diego, CA, USA). Antibodies against GAPDH, ubiquitin, p-Akt/Akt, p-p70S6K/p70S6K, p-AMPK/AMPK and p-mTOR/mTOR were purchased from Cell Signaling. The collagen I antibody was from Abcam. Recombinant rat PDGF was obtained from R&D Biosystems (Minneapolis, MN, USA). Polyclonal antibodies against KLH (keyhole-limpet haemocyanin)–HNE (protein–4-HNE) were raised and tested as previously described [20]. HRP-conjugated rabbit and mouse IgG secondary antibodies were obtained from Cell Signaling Technologies (Danvers, MA, USA). Goat anti-mouse IgG-Alexafluor 555 was obtained from Invitrogen (Grand Island, NY, USA). The 3-methyladenine (3-MA), epoxomicin, and bafilomycin A1 were obtained from Sigma-Aldrich. Spautin-1 was obtained from Cellagen Technology (San Diego, CA, USA). All primers used for real time PCR were designed using the primer express software from Applied Biosystems (Carlsbad, CA, USA) and then ordered from Integrated DNA Technologies (Coralville, IA, USA). DAPI stain was obtained from Invitrogen. Electrophoresis supplies were purchased from Bio-Rad (Hercules, CA, USA). ECL® reagents were purchased from GE Healthcare (Pittsburgh, PA, USA).

Cell culture

Rat aortic smooth muscle cells (VSMCs) were isolated from the aortas of 6-week-old male Sprague-Dawley rats as previously described [21]. Briefly, rat aortas were cleaned of fat and adventitial tissue and then minced in sterile culture dishes. The minced aortas were then digested at 37°C in 5% CO_2 for 1 h in an enzyme solution containing 0.1% collagenase type 1A, 0.05% elastase type III, 2 mg/ml BSA, 2 mM calcium chloride, and 1% penicillin/streptomycin (P/S, Life Technologies – Invitrogen). After the digestion, the supernatant was carefully removed and discarded. The undigested tissue was further digested for up to 3 h with fresh enzyme solution. Growth medium [Dulbecco's modified Eagle's medium (Life Technologies–Invitrogen) containing 10% v/v fetal bovine serum (Atlanta Biologicals, Atlanta, GA, USA), and 1% v/v P/S] was added immediately after all tissue was digested, and the solution was centrifuged for 5 min at 500×*g* at 4°C to pellet cells. The cells were resuspended in growth medium, counted, and plated in a final volume of 2.5 ml at a density of 0.4–0.6×10^6 cells per 25 mm^2 flask.

The purity of VSMCs was verified by flow cytometry using anti-calponin and anti-α-sm actin staining (Supplemental Fig. 1). To ensure maintenance of the contractile phenotype, only cells between passages 2–7 were used. Cells were maintained at 37°C in a humidified atmosphere containing 5% CO_2. At ~70% confluency, VSMCs were serum-starved in DMEM containing 0.1% FBS for 24 h. After desired treatments, cells were rinsed twice with

phosphate-buffered saline and then lysed in a protein lysis buffer containing 25 mM HEPES, 1 mM EDTA, 1 mM EGTA, 0.1% SDS, 1% NP-40, and 1× protease and phosphatase inhibitors. The Lowry DC assay (Biorad, Hercules, CA, USA) was used for measuring protein concentration of crude cell extracts.

Messenger RNA isolation and real-time PCR

Messenger RNA was isolated from VSMCs using TRIzol reagent (Invitrogen) and the concentration was determined by measuring absorbance at 260 nm using a Nanodrop spectrophotometer (Thermo scientific). A 20 μl reverse transcription reaction mixture containing 1 μg mRNA, 10 units AMV reverse transcriptase, 0.4 μM poly T primer (dT18), 0.2 mM dNTPs, and 20 units RNasin (Promega) was subjected to complementary DNA (cDNA) synthesis in a thermal cycler (BioRad). Two microliters of cDNA was then used for amplification of the gene of interest by real time PCR using SYBR green (VWR, Radnor, PA, USA).

Western blotting

Depending on the target protein, 0.5–25 μg of crude cell protein was applied to each lane of a 10.5–14% Bis–Tris-HCl gel and electroblotted onto a PVDF membrane. The membrane was then incubated overnight at 4°C using appropriate dilutions of primary antibodies. PVDF membranes were then incubated at room temperature with horseradish peroxidase-conjugated secondary antibodies. Immunoreactive bands were detected using a Typhoon scanner (SA Biosciences, Valencia, CA, USA) after exposure to ECL detection reagent. Band intensity was quantified by using the TotalLab TL120 software.

Measurement of protein-bound HNE

VSMCs were serum-starved for 24 h and then treated without or with PDGF (20 ng/ml) for 48 h. After PDGF treatment, cells were exposed to 50 μM HNE in HBSS for 30 min and then the medium was replaced with DMEM containing 10% FBS. Cells were then incubated in the HNE-free medium for 3.5 h. Cells were lysed using lysis buffer, and 25 μg used for Western blot to quantify protein-HNE adducts using an anti-protein HNE antibody [20].

LDH activity assay

VSMCs were serum-starved for 24 h and then treated without or with PDGF (20 ng/ml) for 48 h. After PDGF treatment, cells were exposed to 50 μM HNE in HBSS for 30 min and then replaced with DMEM containing 10% FBS. After 16 h, LDH assay was performed as previously described [22].

Adenoviral gene transfection

The GFP-LC3 plasmid was a gift from Roberta Gottlieb. The plasmid was amplified in E. coli, and the GFP-LC3 fragment was excised from the plasmid backbone. The GFP-LC3 adenovirus was then developed at Vector Biolabs (Philadephia, PA). Briefly, the GFP-LC3 construct was cloned into a pAd5-dE1/E3 vector for viral packaging and amplification in HEK293 cells. Ad-GFP without LC3 was used as a control viral vector. Adenoviruses were used at a multiplicity of infection (MOI) of 100, and GFP expression was used to ascertain

transduction efficiency. AdGFP or AdGFP-LC3 transduced cells were then stimulated with PDGF at the indicated times. Before imaging, cells were incubated with DAPI stain for nuclear visualization.

Immunofluorescence staining and confocal imaging

VSMCs were cultured on glass chamber slides or glass-bottomed culture dishes and after the appropriate treatments were washed with PBS and then fixed in cold (–20 °C) methanol for 5 min. The cells were then incubated for 30 min at room temperature (RT) in a blocking solution (5% BSA in PBS) followed by incubation for 1 h with a 1:500 dilution of anti-α-sm-actin primary antibody at RT. A 1:1000-diluted solution of goat anti-mouse IgG Alexa Fluor 555 secondary antibody was used for incubation after treatment with the primary antibody. After three washes with PBS, the cells were stained with DAPI for 10 min at RT. The α-sm-actin staining and GFP-LC3 puncta were visualized using a Nikon TE-2000E2 microscope interfaced with a Nikon A1 confocal system. DAPI was used to visualize nuclei. Prior to imaging live cells, the cells were placed in phenol red-free DMEM supplemented with 25 mmol/L HEPES (pH 7.4). The individual fluorophores were illuminated as indicated below. All images were acquired through a 60× oil-immersion DIC objective (NA=1.4), natively averaged at 2×, scan direction set to one-way, image size was 1024×1024, and channel series was ON. Laser lines were modulated and integrated in the A1's AOTF. For DAPI/GFP imaging, a 405 nm excitation line (Power = 1.1; PMT HV = 80; Offset = 0) with emission collected through a 450/50 nm bandpass filter, and, a 488 nm excitation line (Power = 1.2; PMT HV = 90; Offset = 0) with emission collected through a 525/50 nm bandpass filter were used with a pinhole size of 36.69 μm, scanner zoom set at 1.205, and scan speed was 1. For DAPI/Alexa Fluor 555 (α-sm-actin), a 405 nm excitation line (Power = 2.0; PMT HV = 75; Offset = 0) with emission collected through a 450/50 nm bandpass filter, and, a 561 nm excitation line (Power = 1.1; PMT HV = 90; Offset = 0) with emission collected through a 595/50 nm bandpass filter were used with a pinhole size of 36.07 μm, scanner zoom set at 1.000, and scan speed 1/8.

Migration assay

Migration of VSMCs was measured using the scratch wound assay [23, 24]. Briefly, VSMCs were plated in 96-well cell culture plates and allowed to grow to 70% confluency. The cells were then serum-starved for 24 h in DMEM containing 0.1% FBS and then stimulated with PDGF (20 ng/ml) or vehicle in the absence or presence of spautin-1 (10 μM) for 24 h. A p200 pipet tip was used to create a scratch on the bottom of each well and the cells were incubated further for 24 h. The distance between the edges of the scratch was measured immediately after scratching and again after 24 h. Migration was quantified and expressed as follows: % closure = [(distance immediately after scratching – distance 24 h after scratching) / distance immediately after scratching]×100.

Transmission electron microscopy

VSMCs were grown on cover slips, serum-starved for 24 h, and then treated without or with PDGF (20 ng/ml) for 48 h. The cells were fixed and imaged as described previously [20].

Statistical analysis

Data are mean ± SEM. Multiple groups were compared using one-way ANOVA, followed by Bonferroni post-tests. Unpaired Student's *t* test was used for two-group comparisons. A p value <0.05 was considered significant.

RESULTS

Platelet-derived growth factor induces phenotype switching in VSMCs

To examine the mechanisms regulating the phenotypic transition of VSMCs, we first measured changes in molecular markers of contractile and synthetic VSMC phenotypes. For this, VSMCs were deprived of serum for 24 h to induce cell cycle arrest. The cells were then incubated with vehicle or PDGF-BB (20 ng/ml) for 24 and 48 h. Relative mRNA and protein abundance was measured by RT-PCR and Western blotting, respectively. As shown in Fig. 1A, PDGF treatment for 24 h resulted in a ~50% decrease in the mRNA levels of α-sm-actin and calponin and a robust upregulation of osteopontin (12-fold) and vimentin (2-fold). After 48 h, the levels of α-SMA protein were decreased by 25%, calponin abundance was decreased by 75%, and osteopontin protein was elevated more than 2-fold (Figure 1B and 1C). As observed by immunofluorescence imaging, the α-sm-actin filaments showed marked disorganization in PDGF-treated cells compared with control cells, and this was accompanied by marked changes in cell morphology (Figure 1D). These results confirm previous findings [1, 19, 25] showing that PDGF promotes phenotypic transition of VSMCs.

PDGF induces autophagy in VSMCs

The relatively rapid loss of contractile proteins suggested to us that proteolytic mechanisms may function to remove the contractile apparatus to aid in the transition from the contractile to the synthetic phenotype. Indeed, previous studies have shown that proteasome and calpain inhibitors affect VSMC phenotype [26–28]; however, these studies showed that proteasome inhibition counter-intuitively decreases markers of the contractile phenotype [27], resulting in reduced cell contractility [28]. Therefore, we hypothesized that autophagy may be important for the removal of contractile proteins and protein complexes. To test this hypothesis, we first assessed the effects of PDGF on autophagy in VSMCs by examining LC3-II formation—an indicator of autophagy [29, 30]. As shown in Fig. 2A–C, PDGF stimulation caused a time-dependent increase in LC3-II formation. A significant increase in LC3-II was observed 12 h after PDGF stimulation and maximal increases in LC3-II were obtained 48 h after PDGF treatment, suggesting that PDGF promotes autophagy.

Because the formation of LC3-II is transient and the protein can be rapidly degraded in the lysosome, an increase in LC3-II could also paradoxically indicate a decrease in autophagy. Hence, to more accurately assess autophagic flux, we inhibited the lysosomal degradation of LC3-II by treating cells with bafilomycin A1—an inhibitor of the vacuolar-type H^+-ATPase [30, 31]. As shown in Fig. 2D–F, treatment of control cells with bafilomycin increased LC3-II abundance, which was further increased in PDGF-stimulated cells that were treated with the inhibitor. These data indicate that autophagic flux is higher in PDGF-treated cells. These effects appear to be specific to PDGF because treatment with fibroblast growth factor 1 (FGF-1), a known VSMC mitogen [32], did not affect the abundance of contractile proteins

or increase LC3-II formation, despite increasing cell proliferation to levels similar to that of PDGF (Fig. 2G–J). To obtain further evidence for the induction of autophagy by PDGF, we transduced VSMCs with a GFP-LC3 adenovirus and assessed the formation of punctate LC3, which indicates autophagosomal localization [30]. As shown in Fig. 3A–B, there was a 2-fold increase in fluorescent puncta in PDGF-treated cells, and this was further increased by bafilomycin A1 treatment.

PDGF induces ultrastructural changes and extensive vacuolization in VSMCs

Although LC3-II formation is a validated marker of autophagy, changes in the ultrastructure showing the formation of autophagosomes is considered the “gold-standard” for documenting autophagy. Hence, to examine ultrastructural changes, VSMCs were treated with PDGF for 48 h and then visualized by transmission electron microscopy. Transmission electron micrographs showed that treatment with PDGF (20 ng/ml) for 48 h caused a ~3 fold increase in single-membrane autophagic vacuoles (some containing electron-dense material) as well as early double-membrane vacuoles (Fig. 3D–F), similar to those shown previously [20, 33, 34]. In addition, PDGF treatment resulted in the consistent formation of a singular large double-membrane phagosome per cell (labeled in Figure 3D and E), which may serve as a designated compartment for the digestion of intracellular materials. Collectively, these structural changes are in concordance with our immunological and fluorescence-imaging data and suggest that PDGF is a robust inducer of the autophagic program.

PDGF-induced autophagy occurs via an AMPK- and mTOR-independent mechanism

Activation of autophagy in mammalian cells usually involves the inhibition of the mammalian target of rapamycin (mTOR), an important signaling molecule necessary for the growth and proliferation of cells. During autophagy activation, mTOR is a downstream target of multiple signaling pathways such as the Akt signaling pathway and the AMPK pathway, which inhibit and activate autophagy, respectively. We found that both Akt and mTOR, as well as the substrate of mTOR p70/85S6K, were activated despite the induction of autophagy (Fig. 4A and B). This suggested to us that PDGF-induced autophagy does not occur via inhibition of mTOR. Because AMPK activation was inhibited after PDGF stimulation, PDGF-induced autophagy is likely independent of AMPK activity as well. We also examined whether autophagy induced by PDGF could be due to nutrient starvation. For this, we incubated the cells with PDGF in the absence or presence of excess essential amino acids or pyruvate. As shown in Supplemental Fig. 2, increasing amino acid and pyruvate availability did not affect LC3 expression in PDGF-treated cells, suggesting that this form of autophagy is not due to well-described starvation pathways.

PDGF-induced autophagy is required for phenotype switching

To examine whether autophagy plays a role in VSMC phenotype switching, we pretreated VSMCs with the pharmacological inhibitor of autophagy, 3-methyladenine (3-MA) [35], prior to stimulating the cells with PDGF. As shown in Fig. 5A and B, 3-MA decreased GFP-LC3 puncta formation by more than 50%. This inhibition of autophagy was associated with partial stabilization of the contractile markers calponin and α-sm actin (Fig. 5C–E) and inhibition of smooth muscle cell proliferation (Fig. 5F). We further confirmed the role of autophagy in protein degradation during phenotype switching by using the downstream

inhibitor of autophagy, bafilomycin A1. As shown in Supplemental Fig. 3, bafilomycin, which inhibits the acidification of autophagosomes and the proteolytic degradation of their contents, also prevented the degradation of calponin in PDGF-treated cells.

Because of potential off-target effects of 3-MA [36–38] and the relatively high concentrations of the compound needed to inhibit the autophagic machinery, we tested whether spautin-1, a structurally dissimilar inhibitor of autophagy, would affect VSMC phenotype. Spautin-1 has been recently reported to prevent autophagy by inhibiting the deubiquitinases USP10 and USP13, which leads to beclin 1 and Vps34 (or PI3KIII) degradation [39]. Treatment of VSMCs with spautin-1 (10 μM) prevented PDGF-induced increases in LC3 abundance and prevented losses of calponin and α-SMA after PDGF exposure (Fig. 6A–D). Spautin-1 also prevented PDGF-induced disorganization of actin filaments (Fig. 6E). Interestingly, we did not find changes in the levels of beclin1 and Vps34 in spautin-1-treated cells (Supplemental Fig. 4A–C), suggesting that its mechanism of inhibition of autophagy in VSMCs may be independent of its previously described effect on deubiquitinase activity.

To determine whether the inhibition of autophagy prevents functional changes associated with the synthetic VSMC phenotype, we measured cell proliferation, migration, and the extracellular matrix component collagen I after PDGF treatment in the absence or presence of spautin-1. Similar to that shown with 3-MA (Fig. 5F), spautin-1 prevented PDGF-induced cell proliferation (Fig. 7A). In addition, PDGF-induced migration, as measured by the scratch wound assay [23, 24], was inhibited in spautin-1-treated cells (Fig. 7B,C), as was collagen I synthesis (Fig. 7D,E). Collectively, these results suggest that autophagy is a major regulator of VSMC phenotype and that spautin-1 is particularly effective in preventing conversion to the synthetic phenotype.

To determine if the proteasome plays a role in regulating VSMC phenotype switching, we treated cells with the proteasome inhibitor epoxomicin [40] prior to PDGF treatment and examined contractile protein expression. Although epoxomicin treatment inhibited proteasomal activity, as evidence by the increased abundance of ubiquitinated proteins (Fig. 8A,B), the loss of contractile proteins due to PDGF treatment remained largely unaffected (Fig. 8C–E). Collectively, these results suggest that autophagy, and not proteasomal activity, is required for phenotypic changes in PDGF-stimulated VSMCs.

Synthetic VSMCs are resistant to aldehyde-induced cell death

Lesions in atherosclerotic and restenotic vessels are characterized by increased amounts of proteins modified by lipid peroxidation products such as 4-hydroxy-trans-2-nonenal (4-HNE) [41, 42]. Because previous findings suggest that autophagy prevents toxicity due to 4-HNE [20], we hypothesized that synthetic VSMCs having higher autophagic flux might be protected from 4-HNE-induced cell death. This could be important because synthetic VSMCs are the abundant phenotype found in vascular lesions; hence, their survival may be impacted by their ability to handle oxidative insults. Indeed, as shown in Fig. 9A, cell viability of synthetic VSMCs challenged with HNE was significantly enhanced compared with HNE-challenged contractile VSMCs. Consistent with the role of autophagy in clearing oxidatively damaged proteins [20, 43], synthetic VSMCs resisted accumulation of protein-

HNE adducts due to exogenous HNE exposure (Fig. 9B and C). Inhibiting autophagy with spautin-1 promoted accumulation of HNE-damaged proteins (Fig. 9D and E). These results suggest that PDGF-induced autophagy may be important for promoting the survival of VSMCs found in diseased vessels.

DISCUSSION

The present study demonstrates a novel role for autophagy in regulating VSMC phenotype. We found that PDGF, which promotes the development of the synthetic VSMC phenotype, is a robust inducer of autophagy and that pharmacological inhibition of autophagy by three structurally unrelated inhibitors blocked the degradation of contractile proteins. Spautin-1 was particularly robust in preventing the PDGF-induced synthetic phenotype. This inhibitor of autophagy not only prevented degradation of calponin and α-sm-actin, but it also prevented proliferation, migration, and synthesis of collagen-I after exposure of VSMCs to PDGF. We also found that the synthetic phenotype was more resistant to the electrophilic stress commonly encountered in diseased vessels, and this was associated with an increased ability to remove proteins damaged or modified by electrophiles. These findings uncover PDGF-mediated autophagy as an important regulator of VSMC phenotype and survival.

Previous studies have identified numerous factors that regulate phenotype plasticity in VSMCs. For example, contractile agonists, reactive oxygen species and extracellular matrix components regulate the expression of contractile genes [44–50]. Conversely, growth factors such as PDGF, extracellular matrix components and oxidized phospholipids are known to favor the synthetic phenotype [25, 51–53]. The signaling pathways known to trigger the synthetic phenotype culminate in the displacement of myocardin, a coactivator of serum response factor, from the consensus CArG box upstream of smooth muscle cell marker genes [54]. PDGF is known to act through transcription factors such as KLF4 and Elk-1 as well as microRNAs (such as miR221 and miR222) leading to the displacement of myocardin and downregulation of VSMC contractile genes [55–58]. Hence, most studies to date examined transcriptional and translational changes regulating phenotypic transition.

We posited that one limiting event to transition to the synthetic phenotype would be removal of the contractile apparatus. Degradation of contractile proteins would likely involve the proteasome, autophagy, or both. Interestingly, the proteasome has been shown to play a role in VSMC hyperplasia but not phenotype switching [59, 60]. Paradoxically, inhibitors of the proteasome decrease markers of the contractile phenotype [27] resulting in reduced cell contractility [28]. In our studies, we found that inhibition of the proteasome with epoxomicin had little effect on contractile protein abundance, suggesting that autophagy could be the major proteolytic device employed by the cell to remove contractile proteins.

We found that PDGF promoted a robust form of autophagy characterized by increased LC3-II abundance, augmented autophagic flux, and the formation of autophagosomes and autophagic vacuoles. The induction of autophagy was specific to PDGF: the mitogen FGF, while increasing proliferation to a similar extent as PDGF, did not induce autophagy. While factors such as TNF-α and osteopontin have been shown to promote autophagy in VSMCs [61, 62], there are surprisingly few reports of induction of autophagy by growth factors. In

fibroblasts and cancer cells, connective tissue growth factor activates autophagy and regulates proliferation [63], and transforming growth factor-β activates autophagy in hepatocellular carcinoma cells [64]. In these cases, the induction of autophagy is usually associated with diminished proliferation; however, we found that autophagy may be important for PDGF-mediated hyperproliferation, as inhibition of autophagy with 3-MA or spautin-1 prevented cellular proliferation induced by PDGF. This is consistent with recent literature showing that 3-MA prevents arterial restenosis [65]. The discrepancy in proliferation between the different inhibitors is likely related to their distinct molecular targets. While 3-MA inhibits autophagy via inhibiting the PI3K-Akt pathway [66], which is also important in regulating cell proliferation, spautin-1 has no effect on the Akt pathway (Supplemental Fig. 5) and inhibits autophagy through a distinct mechanism. It is also possible that PDGF-mediated proliferation may not be directly related to induction of autophagy. PDGF-mediated proliferation in SMCs may depend on FGF release and FGFR activation [67], and we show that FGF-1 alone can promote proliferation despite having no effects on autophagy or phenotype switching. Hence, it is possible that PDGF-mediated FGF autocrine effects are retarded when autophagy is inhibited. Additionally, it may be that the decreased generation of metabolic building blocks, e.g., free amino acids—a natural consequence of enhanced autophagic activity—could be used to supply energy requirements for increased proliferation.

The induction of autophagy by PDGF does not appear to be mediated by AMPK or mTOR. Exposure of cells to PDGF resulted in a decrease in the phosphorylation of AMPK and increased phosphorylation of mTOR and its downstream substrates p85- and p70s6k (Fig. 4). Because activation of autophagy due to nutrient deprivation is typically linked to enhanced AMPK phosphorylation or inhibition of mTOR, it is unlikely that these pathways regulate the autophagic program initiated by PDGF. It remains unclear why rapamycin, which is an inhibitor of mTOR and activator of autophagy, promotes the contractile phenotype in VSMCs [68, 69], while PDGF-mediated autophagy induces the synthetic phenotype. It is likely that the form of autophagy induced by PDGF is uniquely poised to degrade contractile proteins and is tailored to regulate the phenotype switch.

Our observation that three structurally distinct inhibitors of autophagy stabilized the contractile phenotype supports the view that autophagy is required for PDGF-induced phenotype conversion. Spautin-1 was most robust in stabilizing the abundance of contractile proteins, and it completely prevented hyperproliferation, migration, and synthesis of collagen-1 after PDGF exposure. The inhibition of autophagy with spautin-1 did not affect PDGF signaling through Akt and Erk (Supplemental Fig. 5), further suggesting that inhibition of phenotype switching was due to stabilization of the contractile apparatus. Interestingly, spautin-1 appeared to inhibit autophagy in a manner different from what has been published previously [39]: spautin-1 treatment did not decrease levels of vps34 or Beclin-1 in VSMCs (Supplemental Fig. 4), despite completely inhibiting PDGF-induced autophagy and preventing phenotype transition. Therefore, the mechanism by which spautin inhibits autophagy in VSMCs remains unclear.

It should be noted that the inhibitors of autophagy used in this study could have autophagy-independent effects that might regulate VSMC phenotype. For example, the effects of

bafilomycin on vesicular trafficking have been shown to inhibit canonical Wnt signaling [70], which is an important regulator of VSMC proliferation, migration, and development [71]. Similarly, it is possible that unidentified, off-target effects of spautin could affect VSMC phenotype. Nevertheless, the findings that all three inhibitors of autophagy, i.e., spautin-1, 3-MA and bafilomycin, prevented PDGF-induced losses of contractile proteins supports the concept that autophagy regulates the contractile-to-synthetic VSMC phenotype transition. Moreover, the remarkable efficacy of spautin-1 for inhibiting PDGF-induced autophagy and preventing phenotype switching *in vitro* suggests that it might be a useful therapeutic agent for preventing phenotype switching and proliferation in certain circumstances of vascular injury, such as restenosis.

In addition to contractile proteins, autophagy has been shown to be important in preventing accumulation of damaged or aggregated proteins [20, 43, 72]. We found that the increase in autophagic flux in PDGF-treated VSMCs was sufficient to decrease cell death and the abundance of protein-HNE adducts after aldehyde challenge, suggesting that PDGF-induced autophagy primes synthetic VSMCs to better tolerate the high levels of HNE [41, 73, 74] and oxidant stress prevalent in vascular lesions. This tolerance may be important for maintaining plaque stability, which would be consistent with findings showing that induction of autophagy in macrophages prevents the accumulation of damaged proteins and stabilizes atherosclerotic plaques [75]. Thus, overall, the promotion of autophagy, cell survival and increased formation of extracellular matrix by PDGF might safeguard plaque-resident VSMCs against oxidative injury while also stabilizing lipid-laden atherosclerotic plaques. Interestingly, the form of autophagy induced by PDGF appears to be functionally different from what has been described to occur with other stimuli. For example, TNF-α and IGF-1 were shown to increase autophagy in VSMCs, yet promote an autophagic form of cell death [61]. Further studies are required to elucidate how apparently divergent forms of autophagy regulate atherosclerosis progression and plaque stability.

In summary, the present study identifies a new mechanism by which autophagy is activated and shows that autophagy is critical for attaining a synthetic VSMC phenotype and for increasing resistance to oxidative stress. Our observations also suggest that therapies targeting autophagy might be useful in preventing aberrant smooth muscle cell growth, but that such interventions may have deleterious effects on synthetic smooth muscle cell survival under conditions of oxidative stress. Future studies are required to identify the detailed molecular mechanism(s) by which PDGF activates the autophagic program and to test how modulating PDGF-mediated autophagy affects the progression of vascular disease.

Supplementary Material

Refer to Web version on PubMed Central for supplementary material.

Acknowledgments

FUNDING

This work was supported by the National Institutes of Health [P20 RR024489, R01 HL083320, R01 HL094419, and P01 HL078825].

Abbreviations

α-sm-actin	alpha-smooth muscle actin
DAPI	4',6-diamidino-2-phenylindole
DMEM	Dulbecco's Modified Eagle Medium
FGF	fibroblast growth factor
FGFR	fibroblast growth factor receptor
HBSS	Hank's Balanced Salt Solution
4-HNE	4-hydroxynonenal
LC3	microtubule-associated protein light chain 3
PDGF	platelet-derived growth factor
VSMC	vascular smooth muscle cell
SP-1	specific and potent inhibitor of autophagy 1 (spautin-1)
3-MA	3-methyl adenine
mTOR	mammalian target of rapamycin
LDH	lactate dehydrogenase
GFP	green fluorescent protein
FBS	fetal bovine serum
BAF	bafilomycin A1
AMPK	AMP-activated protein kinase
TNF-α	tumor necrosis factor alpha
IGF-1	insulin growth factor 1
MTT	3-(4,5-Dimethylthiazol-2-yl)-2,5-diphenyltetrazolium bromide

REFERENCES

1. Owens GK, Kumar MS, Wamhoff BR. Molecular regulation of vascular smooth muscle cell differentiation in development and disease. Physiol. Rev. 2004; 84:767–801. [PubMed: 15269336]
2. Mack CP. Signaling mechanisms that regulate smooth muscle cell differentiation. Arterioscler. Thromb. Vasc. Biol. 2011; 31:1495–1505. [PubMed: 21677292]
3. Pyle AL, Young PP. Atheromas feel the pressure: biomechanical stress and atherosclerosis. Am. J. Pathol. 2010; 177:4–9. [PubMed: 20558573]
4. Ferns GA, Raines EW, Sprugel KH, Motani AS, Reidy MA, Ross R. Inhibition of neointimal smooth muscle accumulation after angioplasty by an antibody to PDGF. Science. 1991; 253:1129–1132. [PubMed: 1653454]
5. Jackson CL, Raines EW, Ross R, Reidy MA. Role of endogenous platelet-derived growth factor in arterial smooth muscle cell migration after balloon catheter injury. Arterioscler. Thromb. 1993; 13:1218–1226. [PubMed: 8343497]
6. Lewis CD, Olson NE, Raines EW, Reidy MA, Jackson CL. Modulation of smooth muscle proliferation in rat carotid artery by platelet-derived mediators and fibroblast growth factor-2. Platelets. 2001; 12:352–358. [PubMed: 11672474]

7. Giese NA, Marijianowski MM, McCook O, Hancock A, Ramakrishnan V, Fretto LJ, Chen C, Kelly AB, Koziol JA, Wilcox JN, Hanson SR. The role of alpha and beta platelet-derived growth factor receptor in the vascular response to injury in nonhuman primates. Arterioscler. Thromb. Vasc. Biol. 1999; 19:900–909. [PubMed: 10195916]
8. Hart CE, Kraiss LW, Vergel S, Gilbertson D, Kenagy R, Kirkman T, Crandall DL, Tickle S, Finney H, Yarranton G, Clowes AW. PDGFbeta receptor blockade inhibits intimal hyperplasia in the baboon. Circulation. 1999; 99:564–569. [PubMed: 9927405]
9. Noiseux N, Boucher CH, Cartier R, Sirois MG. Bolus endovascular PDGFR-beta antisense treatment suppressed intimal hyperplasia in a rat carotid injury model. Circulation. 2000; 102:1330–1336. [PubMed: 10982551]
10. Sirois MG, Simons M, Edelman ER. Antisense oligonucleotide inhibition of PDGFR-beta receptor subunit expression directs suppression of intimal thickening. Circulation. 1997; 95:669–676. [PubMed: 9024156]
11. Leppanen O, Janjic N, Carlsson MA, Pietras K, Levin M, Vargeese C, Green LS, Bergqvist D, Ostman A, Heldin CH. Intimal hyperplasia recurs after removal of PDGF-AB and -BB inhibition in the rat carotid artery injury model. Arterioscler. Thromb. Vasc. Biol. 2000; 20:E89–E95. [PubMed: 11073860]
12. Buetow BS, Tappan KA, Crosby JR, Seifert RA, Bowen-Pope DF. Chimera analysis supports a predominant role of PDGFRbeta in promoting smooth-muscle cell chemotaxis after arterial injury. Am. J. Pathol. 2003; 163:979–984. [PubMed: 12937138]
13. Myllarniemi M, Calderon L, Lemstrom K, Buchdunger E, Hayry P. Inhibition of platelet-derived growth factor receptor tyrosine kinase inhibits vascular smooth muscle cell migration and proliferation. FASEB J. 1997; 11:1119–1126. [PubMed: 9367346]
14. Yamasaki Y, Miyoshi K, Oda N, Watanabe M, Miyake H, Chan J, Wang X, Sun L, Tang C, McMahon G, Lipson KE. Weekly dosing with the platelet-derived growth factor receptor tyrosine kinase inhibitor SU9518 significantly inhibits arterial stenosis. Circ. Res. 2001; 88:630–636. [PubMed: 11282898]
15. Yu JC, Lokker NA, Hollenbach S, Apatira M, Li J, Betz A, Sedlock D, Oda S, Nomoto Y, Matsuno K, Ide S, Tsukuda E, Giese NA. Efficacy of the novel selective platelet-derived growth factor receptor antagonist CT52923 on cellular proliferation, migration, and suppression of neointima following vascular injury. J. Pharmacol. Exp. Ther. 2001; 298:1172–1178. [PubMed: 11504817]
16. Panda D, Kundu GC, Lee BI, Peri A, Fohl D, Chackalaparampil I, Mukherjee BB, Li XD, Mukherjee DC, Seides S, Rosenberg J, Stark K, Mukherjee AB. Potential roles of osteopontin and alphaVbeta3 integrin in the development of coronary artery restenosis after angioplasty. Proc. Natl. Acad. Sci. U.S.A. 1997; 94:9308–9313. [PubMed: 9256478]
17. Palmberg L, Sjolund M, Thyberg J. Phenotype modulation in primary cultures of arterial smooth-muscle cells: reorganization of the cytoskeleton and activation of synthetic activities. Differentiation. 1985; 29:275–283. [PubMed: 2416624]
18. Worth NF, Rolfe BE, Song J, Campbell GR. Vascular smooth muscle cell phenotypic modulation in culture is associated with reorganisation of contractile and cytoskeletal proteins. Cell Motil. Cytoskeleton. 2001; 49:130–145. [PubMed: 11668582]
19. Thyberg J, Palmberg L, Nilsson J, Ksiazek T, Sjolund M. Phenotype modulation in primary cultures of arterial smooth muscle cells. On the role of platelet-derived growth factor. Differentiation. 1983; 25:156–167. [PubMed: 6686563]
20. Hill BG, Haberzettl P, Ahmed Y, Srivastava S, Bhatnagar A. Unsaturated lipid peroxidation-derived aldehydes activate autophagy in vascular smooth-muscle cells. Biochem. J. 2008; 410:525–534. [PubMed: 18052926]
21. Srivastava S, Conklin DJ, Liu SQ, Prakash N, Boor PJ, Srivastava SK, Bhatnagar A. Identification of biochemical pathways for the metabolism of oxidized low-density lipoprotein derived aldehyde-4-hydroxy trans-2-nonenal in vascular smooth muscle cells. Atherosclerosis. 2001; 158:339–350. [PubMed: 11583712]
22. Perez J, Hill BG, Benavides GA, Dranka BP, Darley-Usmar VM. Role of cellular bioenergetics in smooth muscle cell proliferation induced by platelet-derived growth factor. Biochem. J. 2010; 428:255–267. [PubMed: 20331438]

23. Guo X, Nie L, Esmailzadeh L, Zhang J, Bender JR, Sadeghi MM. Endothelial and smooth muscle-derived neuropilin-like protein regulates platelet-derived growth factor signaling in human vascular smooth muscle cells by modulating receptor ubiquitination. J. Biol. Chem. 2009; 284:29376–29382. [PubMed: 19696027]
24. Liang CC, Park AY, Guan JL. In vitro scratch assay: a convenient and inexpensive method for analysis of cell migration in vitro. Nat. Protoc. 2007; 2:329–333. [PubMed: 17406593]
25. Chen CN, Li YS, Yeh YT, Lee PL, Usami S, Chien S, Chiu JJ. Synergistic roles of platelet-derived growth factor-BB and interleukin-1beta in phenotypic modulation of human aortic smooth muscle cells. Proc. Natl. Acad. Sci. U.S.A. 2006; 103:2665–2670. [PubMed: 16477012]
26. Thyberg J, Blomgren K. Effects of proteasome and calpain inhibitors on the structural reorganization and proliferation of vascular smooth muscle cells in primary culture. Lab. Invest. 1999; 79:1077–1088. [PubMed: 10496526]
27. Sandbo N, Qin Y, Taurin S, Hogarth DK, Kreutz B, Dulin NO. Regulation of serum response factor-dependent gene expression by proteasome inhibitors. Mol. Pharmacol. 2005; 67:789–797. [PubMed: 15550677]
28. Yin H, Jiang Y, Li H, Li J, Gui Y, Zheng XL. Proteasomal degradation of myocardin is required for its transcriptional activity in vascular smooth muscle cells. J. Cell. Physiol. 2011; 226:1897–1906. [PubMed: 21506120]
29. Codogno P, Meijer AJ. Autophagy and signaling: their role in cell survival and cell death. Cell Death Differ. 2005; 12:1509–1518. [PubMed: 16247498]
30. Klionsky DJ, Abeliovich H, Agostinis P, Agrawal DK, Aliev G, Askew DS, Baba M, Baehrecke EH, Bahr BA, Ballabio A, Bamber BA, Bassham DC, Bergamini E, Bi XN, Biard-Piechaczyk M, Blum JS, Breclesen DE, Brodsky JL, Brumell JH, Brunk UT, Bursch W, Camougrand N, Cebollero E, Cecconi F, Chen YY, Chin LS, Choi A, Chu CT, Chung JK, Clarke PGH, Clark RSB, Clarke SG, Clave C, Cleveland JL, Codogno P, Colombo MI, Coto-Montes A, Cregg JM, Cuervo AM, Debnath J, Demarchi F, Dennis PB, Dennis PA, Deretic V, Devenish RJ, Di Sano F, Dice JF, DiFiglia M, Dinesh-Kumar S, Distelhorst CW, Djavaheri-Mergny M, Dorsey FC, Droge W, Dron M, Dunn WA, Duszenko M, Eissa NT, Elazar Z, Esclatine A, Eskelinen EL, Fesues L, Finley KD, Fuentes JM, Fueyo J, Fujisaki K, Galliot B, Gao FB, Gewirtz DA, Gibson SB, Gohla A, Goldberg AL, Gonzalez R, Gonzalez-Estevez C, Gorski S, Gottlieb RA, Haussinger D, He YW, Heidenreich K, Hill JA, Hoyer-Hansen M, Hu X, Huang WP, Iwasaki A, Jaattela M, Jackson WT, Jiang X, Jin SK, Johansen T, Jung JU, Kadowaki M, Kang C, Kelekar A, Kessel DH, Kiel JAKW, Kim HP, Kimchi A, Kinsella TJ, Kiselyov K, Kitamoto K, Knecht E, Komatsu M, Kominami E, Konclo S, Kovacs AL, Kroemer G, Kuan CY, Kumar R, Kundu M, Landry J, Laporte M, Le WD, Lei HY, Lenardo MJ, Levine B, Lieberman A, Lim KL, Lin FC, Liou W, Liu LF, Lopez-Berestein G, Lopez-Otin C, Lu B, Macleod KF, Malorni W, Martinet W, Matsuoka K, Mautner J, Meijer AJ, Melendez A, Michels P, Miotto G, Mistiaen WP, Mizushima N, Mograbi B, Monastyrska I, Moore MN, Moreira PI, Moriyasu Y, Motyl T, Munz C, Murphy LO, Naqvi NI, Neufeld TP, Nishino I, Nixon RA, Noda T, Nurnberg B, Ogawa M, Oleinick NL, Olsen LJ, Ozpolat B, Paglin S, Palmer GE, Papassideri I, Parkes M, Perlmutter DH, Perry G, Piacentini M, Pinkas-Kramarski R, Prescott M, Proikas-Cezanne T, Raben N, Rami A, Reggiori F, Rohrer B, Rubinsztein DC, Ryan KM, Sadoshima J, Sakagami H, Sakai Y, Sandri M, Sasakawa C, Sass M, Schneider C, Seglen PO, Seleverstov O, Settleman J, Shacka JJ, Shapiro IM, Sibirny A, Silva-Zacarin ECM, Simon HU, Simone C, Simonsen A, Smith MA, Spanel-Borowski K, Srinivas V, Steeves M, Stenmark H, Stromhaug PE, Subauste CS, Sugimoto S, Sulzer D, Suzuki T, Swanson MS, Takeshita F, Talbot NJ, Talloczy Z, Tanaka K, Tanaka K, Tanida I, Taylor GS, Taylor JP, Terman A, Tettamanti G, Thompson CB, Thumm M, Tolkovsky AM, Tooze SA, Truant R, Tumanovska LV, Uchiyama Y, Ueno T, Uzcategui NL, van der Klei I, Vaquero EC, Vellai T, Vogel MW, Wang HG, Webster P, Wiley JW, Xi ZJ, Xiao G, Yahalom J, Yang JM, Yap G, Yin XM, Yoshimori T, Yu L, Yue ZY, Yuzaki M, Zabirnyk O, Zheng XX, Zhu X, Deter RL, Tabas I. Guidelines for the use and interpretation of assays for monitoring autophagy in higher eukaryotes. Autophagy. 2008; 4:151–175. [PubMed: 18188003]
31. Klionsky DJ, Elazar Z, Seglen PO, Rubinsztein DC. Does bafilomycin A1 block the fusion of autophagosomes with lysosomes? Autophagy. 2008; 4:849–950. [PubMed: 18758232]
32. Lindner V, Lappi DA, Baird A, Majack RA, Reidy MA. Role of basic fibroblast growth factor in vascular lesion formation. Circ. Res. 1991; 68:106–113. [PubMed: 1984855]

33. Martinet W, De Meyer GR, Timmermans JP, Herman AG, Kockx MM. Macrophages but not smooth muscle cells undergo benzyloxycarbonyl-Val-Ala-DL-Asp(O-Methyl)-fluoromethylketone-induced nonapoptotic cell death depending on receptor-interacting protein 1 expression: implications for the stabilization of macrophage-rich atherosclerotic plaques. J. Pharmacol. Exp. Ther. 2006; 317:1356–1364. [PubMed: 16537794]
34. Xu K, Yang Y, Yan M, Zhan J, Fu X, Zheng X. Autophagy plays a protective role in free cholesterol overload-induced death of smooth muscle cells. J. Lipid Res. 2010; 51:2581–2590. [PubMed: 20484746]
35. Seglen PO, Gordon PB. 3-Methyladenine: specific inhibitor of autophagic/lysosomal protein degradation in isolated rat hepatocytes. Proc. Natl. Acad. Sci. U.S.A. 1982; 79:1889–1892. [PubMed: 6952238]
36. Xue LZ, Fletcher GC, Tolkovsky AM. Autophagy is activated by apoptotic signalling in sympathetic neurons: An alternative mechanism of death execution. Mol. Cell. Neurosci. 1999; 14:180–198. [PubMed: 10576889]
37. Blommaart EFC, Krause U, Schellens JPM, VreelingSindelarova H, Meijer AJ. The phosphatidylinositol 3-kinase inhibitors wortmannin and LY294002 inhibit autophagy in isolated rat hepatocytes. Eur. J. Biochem. 1997; 243:240–246. [PubMed: 9030745]
38. Ito S, Koshikawa N, Mochizuki S, Takenaga K. 3-methyladenine suppresses cell migration and invasion of HT1080 fibrosarcoma cells through inhibiting phosphoinositide 3-kinases independently of autophagy inhibition. Int. J. Oncol. 2007; 31:261–268. [PubMed: 17611681]
39. Liu JL, Xia HG, Kim M, Xu LH, Li Y, Zhang LH, Cai Y, Norberg HV, Zhang T, Furuya T, Jin MZ, Zhu ZM, Wang HC, Yu J, Li YX, Hao Y, Choi A, Ke HM, Ma DW, Yuan JY. Beclin1 Controls the Levels of p53 by Regulating the Deubiquitination Activity of USP10 and USP13. Cell. 2011; 147:223–234. [PubMed: 21962518]
40. Meng L, Mohan R, Kwok BH, Elofsson M, Sin N, Crews CM. Epoxomicin, a potent and selective proteasome inhibitor, exhibits in vivo antiinflammatory activity. Proc. Natl. Acad. Sci. U.S.A. 1999; 96:10403–10408. [PubMed: 10468620]
41. Jurgens G, Chen Q, Esterbauer H, Mair S, Ledinski G, Dinges HP. Immunostaining of human autopsy aortas with antibodies to modified apolipoprotein B and apoprotein(a). Arterioscler. Thromb. 1993; 13:1689–1699. [PubMed: 7692957]
42. Palinski W, Ord VA, Plump AS, Breslow JL, Steinberg D, Witztum JL. ApoE-deficient mice are a model of lipoprotein oxidation in atherogenesis. Demonstration of oxidation-specific epitopes in lesions and high titers of autoantibodies to malondialdehyde-lysine in serum. Arterioscler. Thromb. 1994; 14:605–616. [PubMed: 7511933]
43. Higdon AN, Benavides GA, Chacko BK, Ouyang X, Johnson MS, Landar A, Zhang J, Darley-Usmar VM. Hemin causes mitochondrial dysfunction in endothelial cells through promoting lipid peroxidation: the protective role of autophagy. Am. J. Physiol. Heart Circ. Physiol. 2012; 302:H1394–H1409. [PubMed: 22245770]
44. Garat C, Van Putten V, Refaat ZA, Dessev C, Han SY, Nemenoff RA. Induction of smooth muscle alpha-actin in vascular smooth muscle cells by arginine vasopressin is mediated by c-Jun amino-terminal kinases and p38 mitogen-activated protein kinase. J. Biol. Chem. 2000; 275:22537–22543. [PubMed: 10807920]
45. Hautmann MB, Thompson MM, Swartz EA, Olson EN, Owens GK. Angiotensin II-induced stimulation of smooth muscle alpha-actin expression by serum response factor and the homeodomain transcription factor. Circ. Res. 1997; 81:600–610. [PubMed: 9314842]
46. Higashita R, Li L, Van Putten V, Yamamura Y, Zarinetchi F, Heasley L, Nemenoff RA. Galpha16 mimics vasoconstrictor action to induce smooth muscle alpha-actin in vascular smooth muscle cells through a Jun-NH2-terminal kinase-dependent pathway. J. Biol. Chem. 1997; 272:25845–25850. [PubMed: 9325315]
47. Pickering JG. Regulation of vascular cell behavior by collagen - Form is function. Circ. Res. 2001; 88:458–459. [PubMed: 11249867]
48. Thyberg J, Hultgardhnilsson A. Fibronectin and the Basement-Membrane Components Laminin and Collagen Type-Iv Influence the Phenotypic Properties of Subcultured Rat Aortic Smooth-Muscle Cells Differently. Cell. Tissue Res. 1994; 276:263–271. [PubMed: 8020062]

49. Su B, Mitra S, Gregg H, Flavahan S, Chotani MA, Clark KR, Goldschmidt-Clermont PJ, Flavahan NA. Redox regulation of vascular smooth muscle cell differentiation. Circ. Res. 2001; 89:39–46. [PubMed: 11440976]
50. Wang L, Zheng JG, Du YY, Huang YQ, Li J, Liu B, Liu CJ, Zhu Y, Gao YS, Xu QB, Kong W, Wang X. Cartilage Oligomeric Matrix Protein Maintains the Contractile Phenotype of Vascular Smooth Muscle Cells by Interacting With alpha(7)beta(1) Integrin. Circ Res. 2010; 106:514–525. [PubMed: 20019333]
51. Pidkovka NA, Cherepanova OA, Yoshida T, Alexander MR, Deaton RA, Thomas JA, Leitinger N, Owens GK. Oxidized phospholipids induce phenotypic switching of vascular smooth muscle cells in vivo and in vitro. Circ. Res. 2007; 101:792–801. [PubMed: 17704209]
52. Wang L, Zheng J, Bai X, Liu B, Liu CJ, Xu QB, Zhu Y, Wang NP, Kong W, Wang X. ADAMTS-7 Mediates Vascular Smooth Muscle Cell Migration and Neointima Formation in Balloon-Injured Rat Arteries. Circ. Res. 2009; 104 688-U247.
53. Millette E, Rauch BH, Defawe O, Kenagy RD, Daum G, Clowes AW. Platelet-derived growth factor-BB-induced human smooth muscle cell proliferation depends on basic FGF release and FGFR-1 activation. Circ. Res. 2005; 96:172–179. [PubMed: 15625285]
54. Yoshida T, Owens GK. Molecular determinants of vascular smooth muscle cell diversity. Circ. Res. 2005; 96:280–291. [PubMed: 15718508]
55. Davis BN, Hilyard AC, Nguyen PH, Lagna G, Hata A. Induction of MicroRNA-221 by Platelet-derived Growth Factor Signaling Is Critical for Modulation of Vascular Smooth Muscle Phenotype. J. Biol. Chem. 2009; 284:3728–3738. [PubMed: 19088079]
56. Liu XJ, Cheng YH, Zhang S, Lin Y, Yang J, Zhang CX. A Necessary Role of miR-221 and miR-222 in Vascular Smooth Muscle Cell Proliferation and Neointimal Hyperplasia. Circ. Res. 2009; 104 476-U125.
57. Yoshida T, Kaestner KH, Owens GK. Conditional deletion of Kruppel-like factor 4 delays downregulation of smooth muscle cell differentiation markers but accelerates neointimal formation following vascular injury. Circ. Res. 2008; 102:1548–1557. [PubMed: 18483411]
58. Yoshida T, Gan Q, Owens GK. Kruppel-like factor 4, Elk-1, and histone deacetylases cooperatively suppress smooth muscle cell differentiation markers in response to oxidized phospholipids. Am. J. Physiol. Cell. Physiol. 2008; 295:C1175–C1182. [PubMed: 18768922]
59. Meiners S, Laule M, Rother W, Guenther C, Prauka I, Muschick P, Baumann G, Kloetzel PM, Stangl K. Ubiquitin-proteasome pathway as a new target for the prevention of restenosis. Circulation. 2002; 105:483–489. [PubMed: 11815432]
60. Demasi M, Laurindo FR. Physiological and pathological role of the ubiquitin-proteasome system in the vascular smooth muscle cell. Cardiovasc. Res. 2012; 95:183–93. [PubMed: 22451513]
61. Jia G, Cheng G, Gangahar DM, Agrawal DK. Insulin-like growth factor-1 and TNF-alpha regulate autophagy through c-jun N-terminal kinase and Akt pathways in human atherosclerotic vascular smooth cells. Immunol. Cell. Biol. 2006; 84:448–454. [PubMed: 16942488]
62. Zheng YH, Tian C, Meng Y, Qin YW, Du YH, Du J, Li HH. Osteopontin stimulates autophagy via integrin/CD44 and p38 MAPK signaling pathways in vascular smooth muscle cells. J. Cell. Physiol. 2012; 227:127–135. [PubMed: 21374592]
63. Capparelli C, Whitaker-Menezes D, Guido C, Balliet R, Pestell TG, Howell A, Sneddon S, Pestell RG, Martinez-Outschoorn U, Lisanti MP, Sotgia F. CTGF drives autophagy, glycolysis and senescence in cancer-associated fibroblasts via HIF1 activation, metabolically promoting tumor growth. Cell Cycle. 2012; 11:2272–2284. [PubMed: 22684333]
64. Kiyono K, Suzuki HI, Matsuyama H, Morishita Y, Komuro A, Kano MR, Sugimoto K, Miyazono K. Autophagy is activated by TGF-beta and potentiates TGF-beta-mediated growth inhibition in human hepatocellular carcinoma cells. Cancer Res. 2009; 69:8844–8852. [PubMed: 19903843]
65. Li H, Li J, Li Y, Singh P, Cao L, Xu LJ, Li D, Wang Y, Xie Z, Gui Y, Zheng XL. Sonic hedgehog promotes autophagy of vascular smooth muscle cells. Am. J. Physiol. Heart Circ. Physiol. 2012; 303:H1319–H1331. [PubMed: 23023870]
66. Petiot A, Ogier-Denis E, Blommaart EF, Meijer AJ, Codogno P. Distinct classes of phosphatidylinositol 3'-kinases are involved in signaling pathways that control macroautophagy in HT-29 cells. J. Biol. Chem. 2000; 275:992–998. [PubMed: 10625637]

67. Millette E, Rauch BH, Defawe O, Kenagy RD, Daum G, Clowes AW. Platelet-derived growth factor-BB-induced human smooth muscle cell proliferation depends on basic FGF release and FGFR-1 activation. Circ. Res. 2005; 96:172–179. [PubMed: 15625285]
68. Martin KA, Merenick BL, Ding M, Fetalvero KM, Rzucidlo EM, Kozul CD, Brown DJ, Chiu HY, Shyu M, Drapeau BL, Wagner RJ, Powell RJ. Rapamycin promotes vascular smooth muscle cell differentiation through insulin receptor substrate-1/phosphatidylinositol 3-kinase/Akt2 feedback signaling. J. Biol. Chem. 2007; 282:36112–36120. [PubMed: 17908691]
69. Ding M, Xie Y, Wagner RJ, Jin Y, Carrao AC, Liu LS, Guzman AK, Powell RJ, Hwa J, Rzucidlo EM, Martin KA. Adiponectin Induces Vascular Smooth Muscle Cell Differentiation via Repression of Mammalian Target of Rapamycin Complex 1 and FoxO4. Arterioscl. Throm. Vas. 2011; 31 1403-U1366.
70. George A, Leahy H, Zhou J, Morin PJ. The vacuolar-ATPase inhibitor bafilomycin and mutant VPS35 inhibit canonical Wnt signaling. Neurobiol. Dis. 2007; 26:125–133. [PubMed: 17239604]
71. Mill C, George SJ. Wnt signalling in smooth muscle cells and its role in cardiovascular disorders. Cardiovasc. Res. 2012; 95:233–240. [PubMed: 22492675]
72. Tannous P, Zhu H, Nemchenko A, Berry JM, Johnstone JL, Shelton JM, Miller FJ Jr, Rothermel BA, Hill JA. Intracellular protein aggregation is a proximal trigger of cardiomyocyte autophagy. Circulation. 2008; 117:3070–3078. [PubMed: 18541737]
73. Salomon RG, Kaur K, Podrez E, Hoff HF, Krushinsky AV, Sayre LM. HNE-derived 2-pentylpyrroles are generated during oxidation of LDL, are more prevalent in blood plasma from patients with renal disease or atherosclerosis, and are present in atherosclerotic plaques. Chem. Res. Toxicol. 2000; 13:557–564. [PubMed: 10898587]
74. Srivastava S, Vladykovskaya E, Barski OA, Spite M, Kaiserova K, Petrash JM, Chung SS, Hunt G, Dawn B, Bhatnagar A. Aldose reductase protects against early atherosclerotic lesion formation in apolipoprotein E-null mice. Circ. Res. 2009; 105:793–802. [PubMed: 19729598]
75. Liao X, Sluimer JC, Wang Y, Subramanian M, Brown K, Pattison JS, Robbins J, Martinez J, Tabas I. Macrophage autophagy plays a protective role in advanced atherosclerosis. Cell. Metab. 2012; 15:545–553. [PubMed: 22445600]

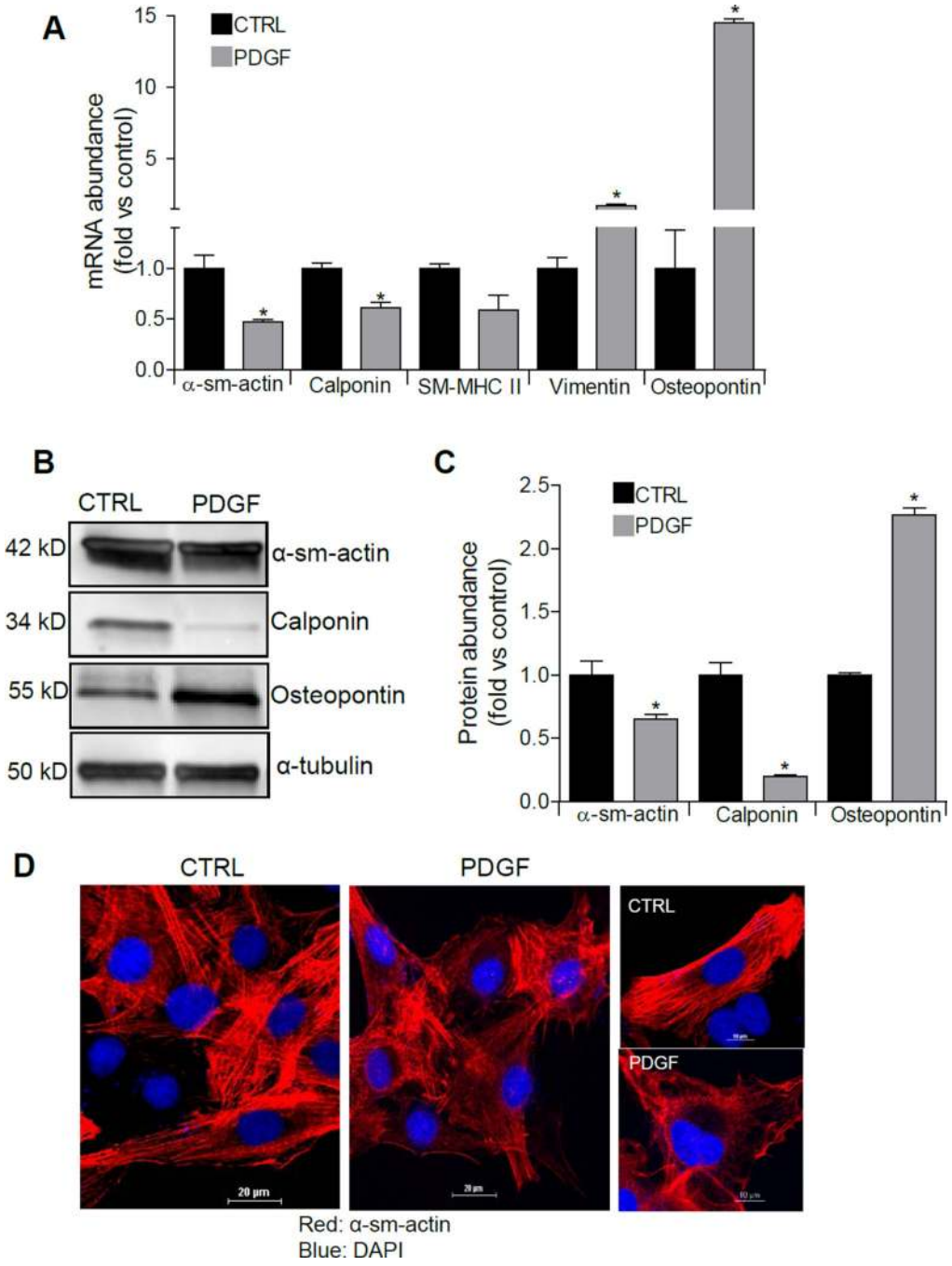

Figure 1. PDGF induces a contractile-to-synthetic phenotype switch in VSMCs

Indices of vascular smooth muscle cell phenotype: **A)** Quantitative real-time PCR following PDGF-BB (20 ng/ml) stimulation for 24 h. Calponin, α-sm-actin and MHC II are markers of the contractile phenotype; osteopontin and vimentin are associated with a synthetic phenotype. *p<0.05 vs. control, n=3 per group. **B)** Western analysis of contractile and synthetic proteins after PDGF stimulation: VSMCs were serum-starved for 24 h and then stimulated with PDGF for 48 h, and, depending on the target protein, 0.5–2 μg protein was used for immunoblot analysis. **C)** Quantification of immunoblots from panel B (*p<0.05 vs

control, n=3 per group). **D)** Confocal images of α-sm-actin (red) distribution in VSMCs treated without (CTRL) and with PDGF (20 ng/ml) for 48 h (Scale bar = 20 μm); note the change in cell morphology upon PDGF treatment (right panels, scale bar = 10 μm). Blue staining (DAPI) indicates nuclei.

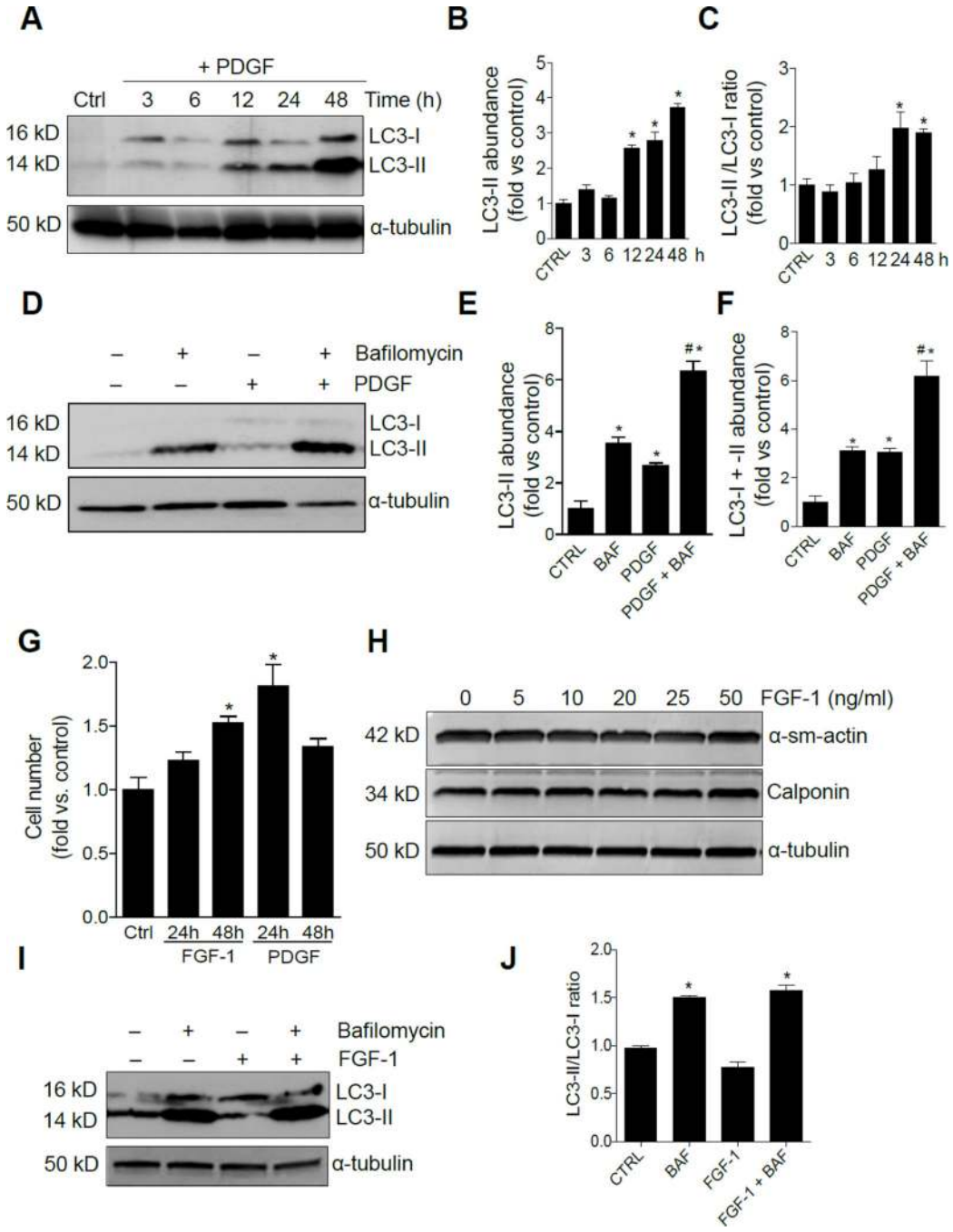

Figure 2. PDGF-BB induces autophagy in VSMCs

Immunoblot analysis: **A)** VSMCs were stimulated with PDGF for 24 h and abundance of LC3 was detected by Western blotting; **B,C)** Quantification of LC3 from panel A. *p<0.05 vs control group, n = 3 per group; **D)** Measurements of autophagic flux: Bafilomycin A1 (0.05 μM) was added to control or PDGF-stimulated cells 1 h prior to harvest, and accumulation of LC3-II was measured by Western blotting; **E,F)** Quantification of LC3 from panel D. *p<0.05 vs. the indicated group, n=3 per group. *p<0.05 vs. CTRL, #p<0.05 vs. BAF or vs. PDGF+BAF; and **G–J)** Effects of FGF-1 on proliferation, contractile protein

abundance, and autophagic flux in VSMCs: panel G, comparison of VSMC proliferation when treated with FGF-1 (25 ng/ml) and PDGF-BB (25 ng/ml) for the indicated times. Cells were counted at the end of the treatment period using a hemocytometer. Panel H, representative western blots of contractile proteins in cells treated with FGF-1 (0–50 ng/ml); Panel I, representative western blot of autophagic flux in untreated and FGF-1-treated cells. Note that bafilomycin (2 μM) was added 4 h prior to cell harvest. Panel J, densitometry measurements of LC3 from panel H. *$p<0.05$ vs. control group, n = 3 per group.

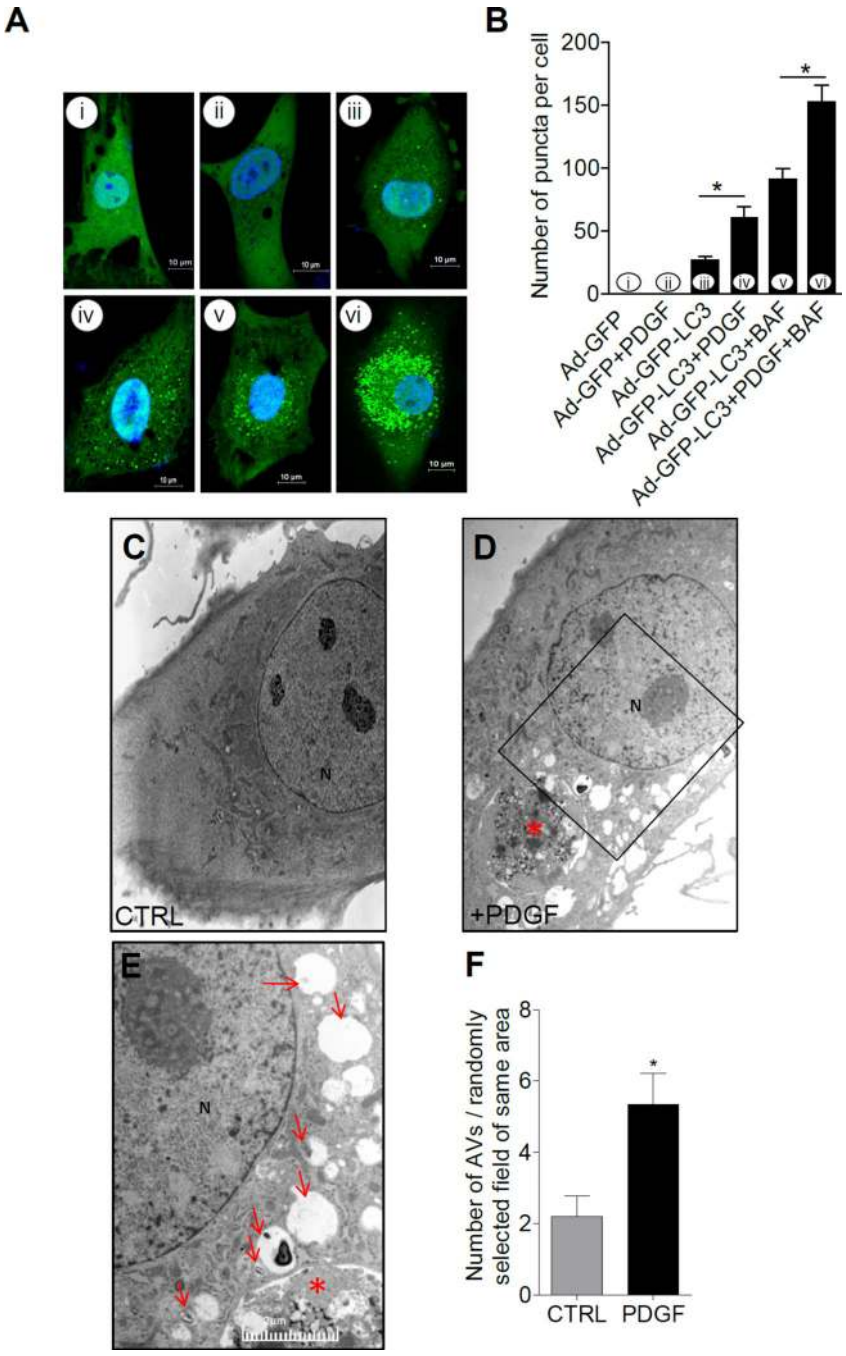

Figure 3. PDGF-BB increases autophagosome formation and promotes extensive vacuolization

Microscopic evaluation of autophagy and VSMC ultrastructure: **A)** Representative confocal images of VSMCs transfected with Ad-GFP (i and ii) or Ad-GFP-LC3 (iii, iv, v, and iv) treated without or with PDGF and/or bafilomycin; **B)** Quantification of puncta in panel B (> 20 cells counted per field in each group, *p<0.01 vs. the indicated groups; **C–E)** Representative transmission electron micrographs of cells treated with vehicle (panel C) or PDGF (panel D) for 48 h. **E**) Magnified image of boxed area in panel D. Light red arrows indicate autophagic vacuoles or early double membrane structures. The large

heterolysosome/phagosome is indicated by the asterisk. N=nucleus. Magnification = ×7100. **F)** Quantification of autophagosomes in images from control and PDGF treatment groups. *p<0.05 vs. CTRL.

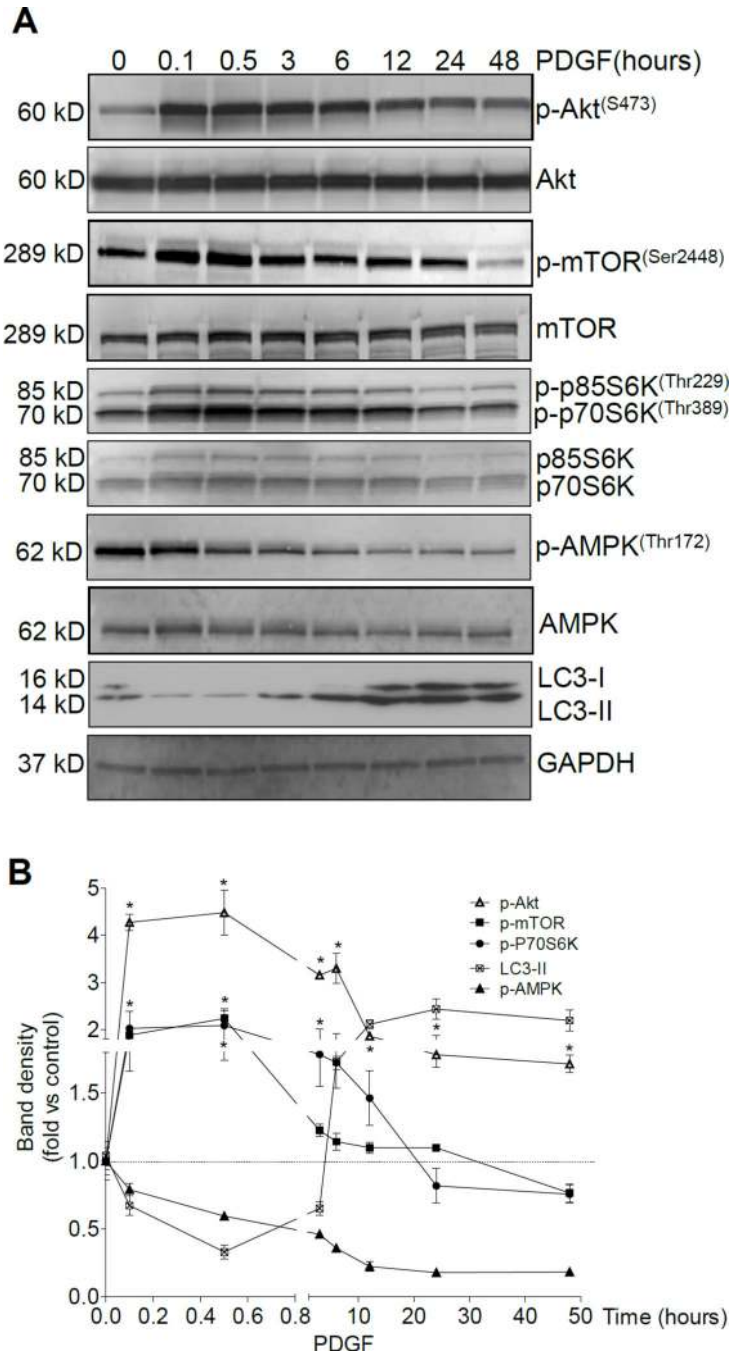

Figure 4. PDGF-induced autophagy is AMPK and mTOR independent

Immunoblot analysis of VSMCs after PDGF treatment: **A)** Representative Western blots of Akt, mTOR, pS6K, and AMPK phosphorylation as well as LC3. Each phospho protein was normalized to its non-phosphorylated total protein band intensity. **B)** Quantification of changes in band intensity from groups shown in panel A. *p<0.05 vs. the 0 hour time point, n=3 per group.

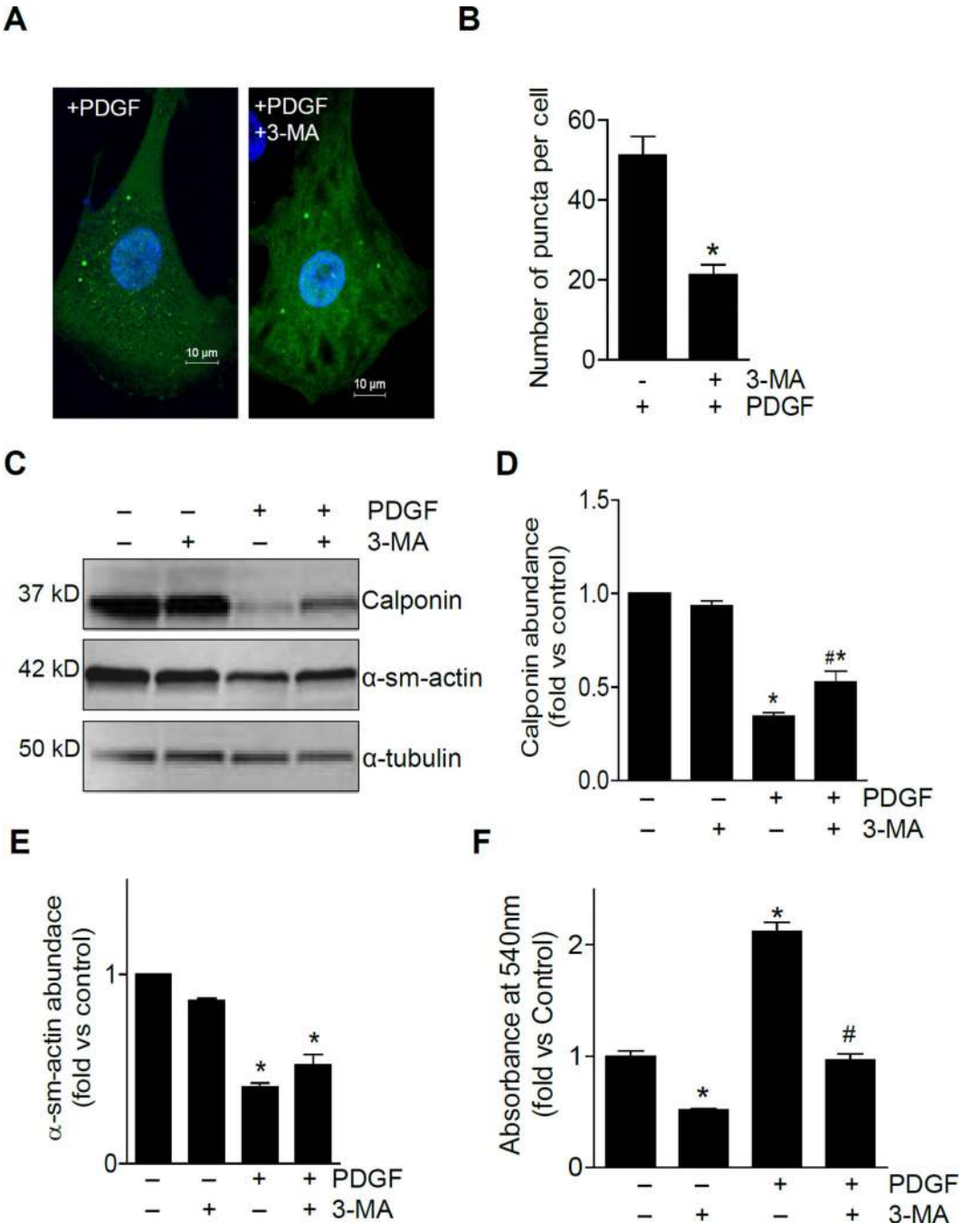

Figure 5. Inhibition of autophagy prevents PDGF-induced phenotype switching

Measurements of autophagy and contractile phenotype in cells treated with 3-methyladenine (3-MA): **A)** Representative confocal images of VSMCs transduced with AdGFP-LC3 and treated with PDGF in the absence or presence of 3-MA (10 mM). **B)** Quantification of fluorescent puncta from panel A. *p<0.03, n=10 cells per group. **C)** Western analysis of contractile protein expression. VSMCs were serum-starved for 24 h and then stimulated with PDGF (20 ng/ml) for 48 hours. 3-MA (10 mM) was added 30 min prior to PDGF stimulation. **D–E)** Quantification of immunoblots represented in panel C. **F)** Cell number

estimation: VSMCs were treated with vehicle or PDGF in the absence or presence of 3-MA. After 48 h, the number of viable cells was estimated using 3-(4,5-dimethylthiazol-2-yl)-2,5-diphenyl-2*H*-tetrazolium bromide (MTT). *$p<0.05$ vs. control and $^{\#}p<0.05$ vs. cells treated with PDGF only, n=3 per group.

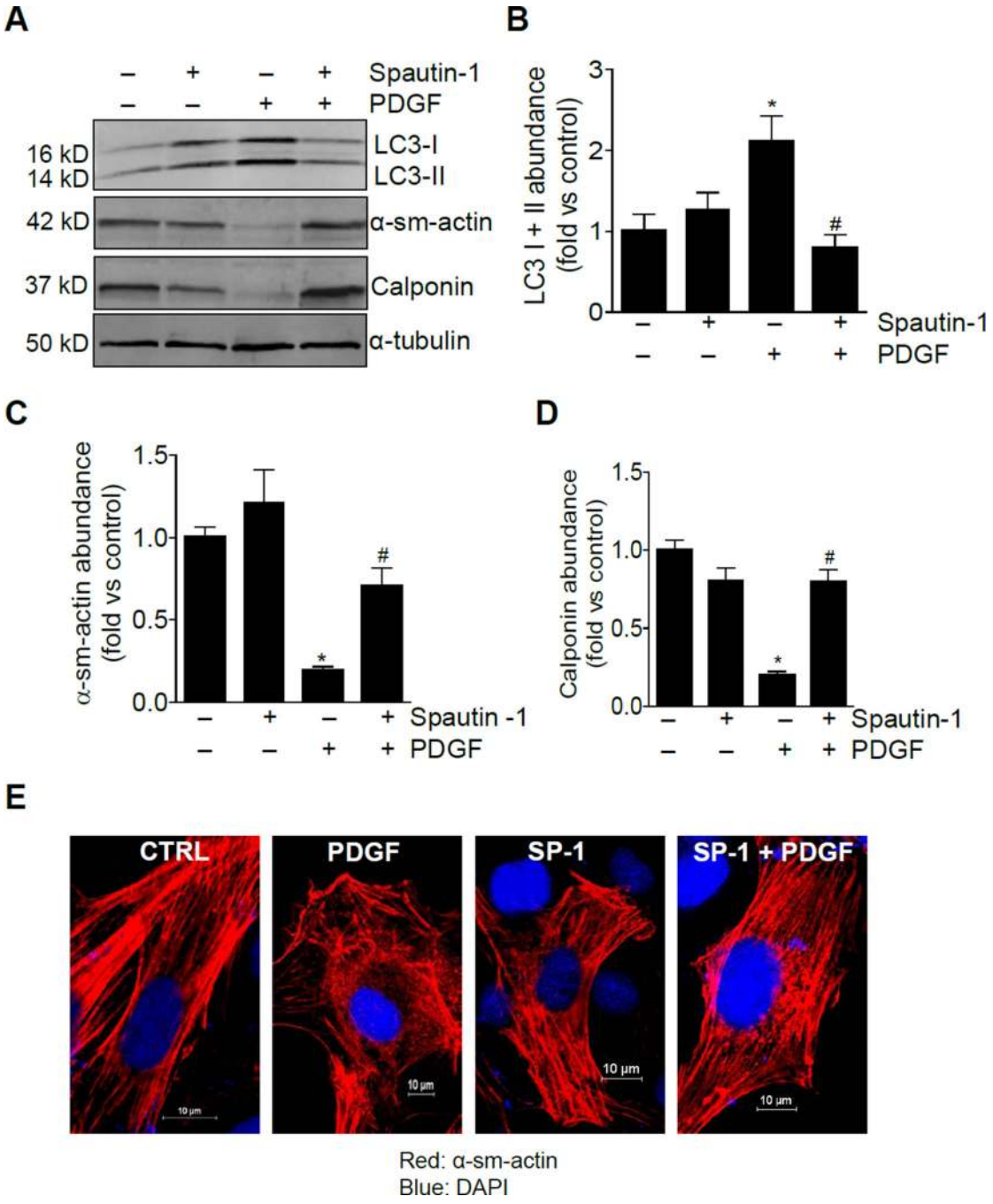

Figure 6. Spautin-1, an inhibitor of autophagy, prevents PDGF-induced phenotype switching

A) Representative Western blots of LC3 and contractile proteins. **B–D)** Quantification of immunoblots from panel A. n = 3 per group, *p<0.05 vs. untreated cells, #p<0.05 vs. cells treated with PDGF only. **E)** Representative confocal images of VSMCs treated without or with PDGF (20 ng/ml) in the absence or presence of spautin-1 (10 μM). Scale bar = 10 μm.

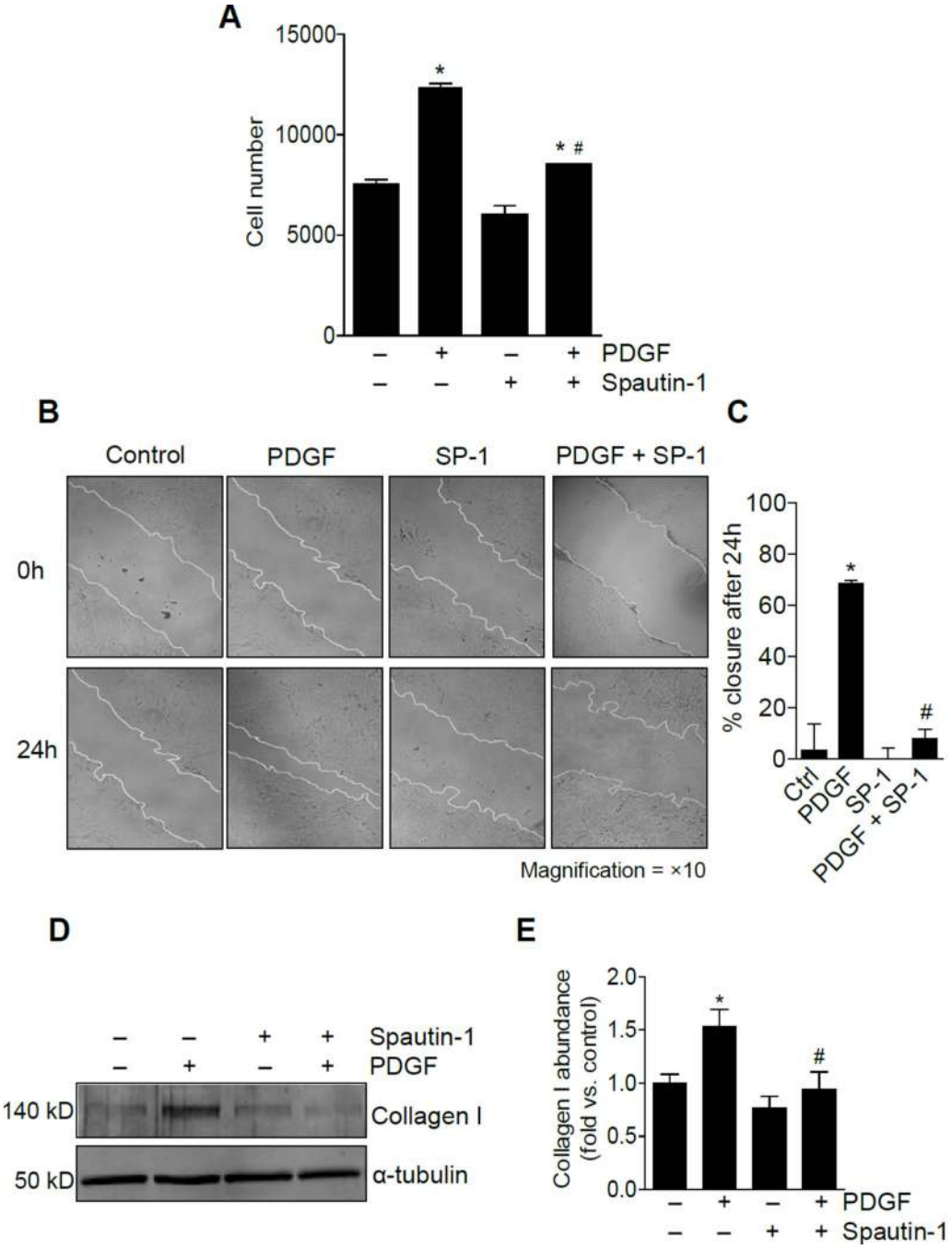

Figure 7. Spautin-1 prevents the functional characteristics of the synthetic phenotype typically induced by PDGF

Proliferation, migration and extracellular matrix production in VSMCs: **A)** Cell proliferation in VSMCs: VSMCs were treated with vehicle or PDGF in the absence or presence of spautin-1. After 48 h, the cells were trypsinized and counted using a hemocytometer. *p<0.05 vs. control; #p<0.05 vs. PDGF alone, n=3 per group. **B)** Cell migration assay: VSMCs were serum-starved for 24 h and then treated as described in the Experimental Methods. **C)** Quantification of B; *p<0.05 vs control, n = 6 per treatment group. **D)**

Regulation of PDGF-induced collagen I synthesis by spautin-1: VSMCs were serum-starved for 24 h and then treated with PDGF (20 ng/ml) in the absence or presence of spautin-1 (10 μM) for 48 h. **E)** Quantification of blots represented in panel D; *$p<0.05$ vs. control, $^{\#}p<0.05$ vs PDGF, n=3 per group.

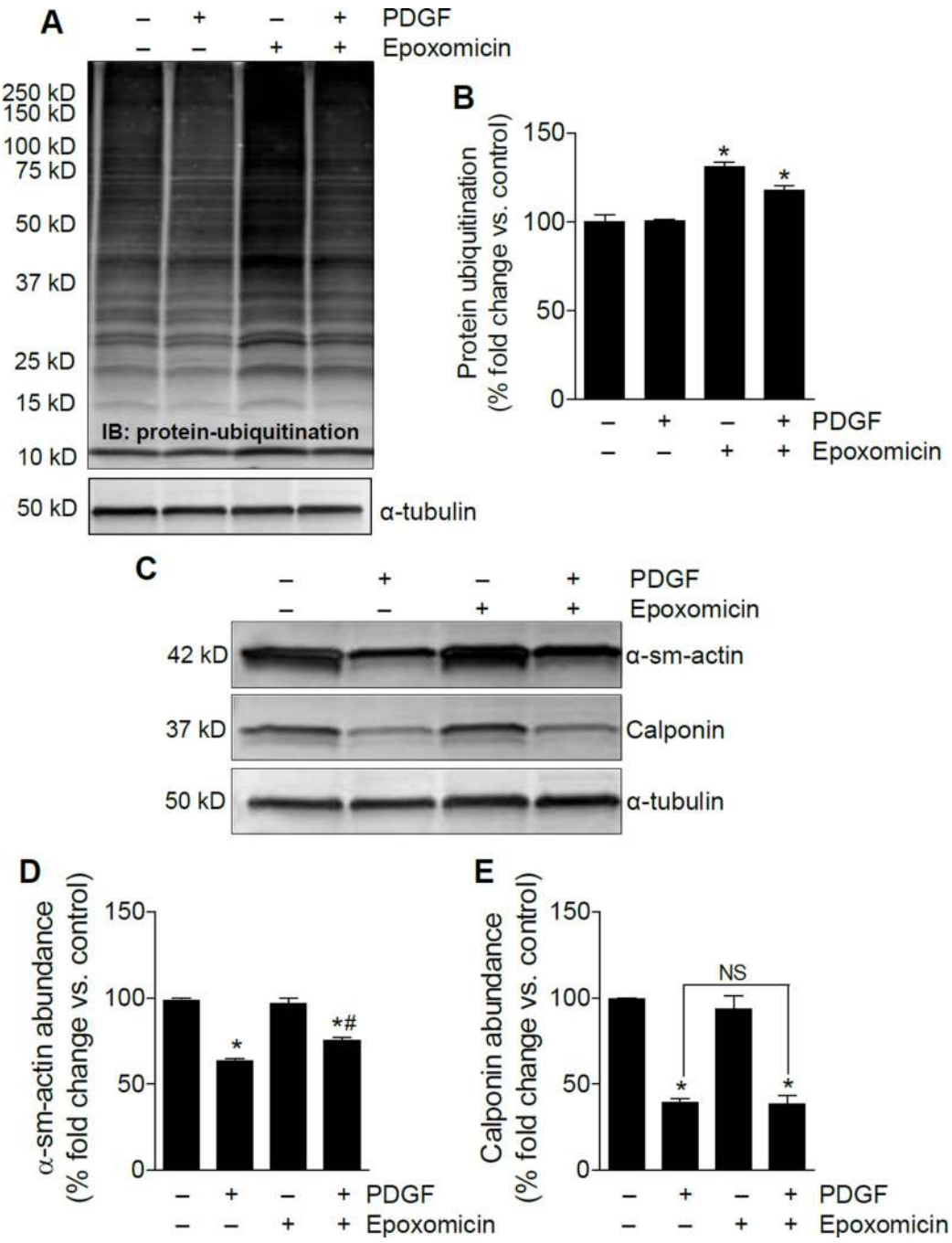

Figure 8. Inhibition of the proteasomal pathway does not affect contractile protein abundance in PDGF-treated cells

Immunoblot analysis of ubiquitinated proteins and contractile proteins: **A)** Accumulation of ubiquitinated proteins after epoxomicin (100 nM) treatment; **B)** Quantification of A; n=3 per group, *p<0.05 vs. control. **C–E)** Effects of epoxomicin on calponin and α-sm-actin abundance: C) Representative western blots; D–E) quantification of C; n=3 per group, *p<0.05 vs. control, #p<0.05 vs. cells treated with PDGF alone.

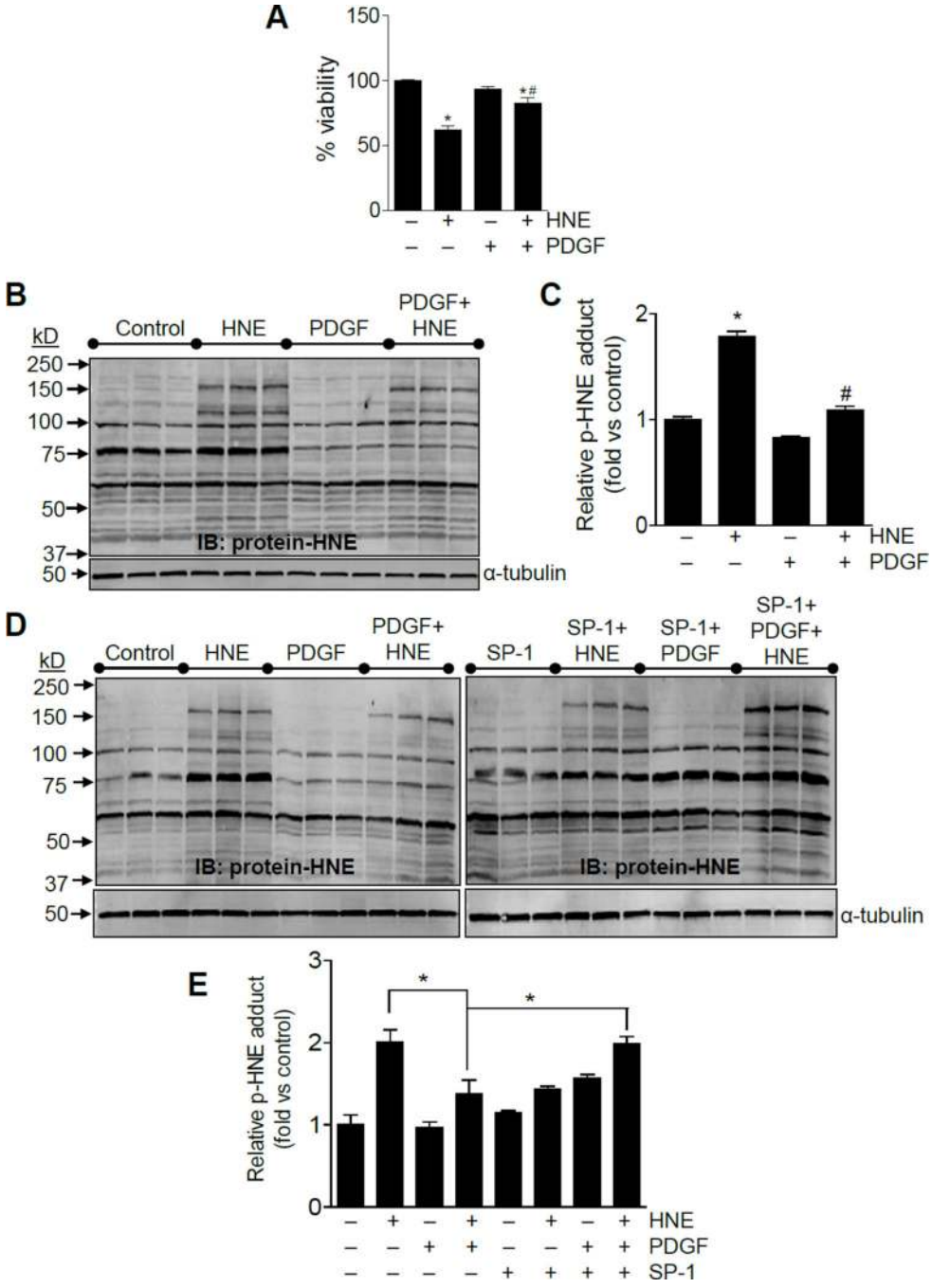

Figure 9. Synthetic VSMCs are resistant to HNE-induced toxicity

A) Cell viability in HNE-treated cells: VSMCs were treated with vehicle or PDGF for 48 h and then exposed to HNE (50 μM) for 30 min in HBSS. The HNE-containing medium was removed and replaced with growth medium, and cell viability was assessed by LDH assay 16 h later. *$p<0.05$ vs. control, $^{\#}p<0.05$ vs. cells treated with HNE alone, n=3 per group. **B,C)** Protein-HNE adduct formation in contractile (control) and synthetic (PDGF-treated) cells: The cells were treated with HNE (50 μM) for 30 min in HBSS. The medium was then replaced with growth medium and the cells were harvested after 3.5 h for examination of

HNE adducts. Representative protein-HNE blots are shown in panel B and quantification is shown in panel C. *p<0.05 vs. control, #p<0.05 vs. cells treated with HNE alone, n=3 per treatment group. **D)** Representative immunoblots of protein-HNE adducts in contractile and synthetic VSMCs treated without (left panel) or with spautin-1 (right panel). **E)** Quantification of groups shown in panel D. All densitometric measurements were normalized to α-tubulin. *p<0.05 vs. the indicated groups, n=3 per group.